Journal of Sound and Vibration (2002) **249**(5), 921–937
doi:10.1006/jsvi.2001.3932, available online at http://www.idealibrary.com on IDEAL®

DYNAMIC TRACTION VECTOR FIELD ESTIMATION IN A STRUCTURE USING HYBRID STRAIN ANALYSIS

N. SEHLSTEDT

Aeronautics Division, FFA, Swedish Defence Research Agency, P.O. Box 11021, *SE*-161 11 *Bromma, Sweden. E-mail: stn@foi.se*

(*Received* 22 *January* 2001, *and in final form* 22 *June* 2001)

The three-dimensional dynamic traction vector of a vibrating structure is obtained with the aid of the so-called hybrid strain analysis. Hybrid strain analysis is a method where vibration response measured at a limited number of points and numerically approximated continuous Hilbert space basis functions combined with spatial differentiation yields the frequency-dependent strain tensor field in a vibrating structure.

Here, an extension and special application of hybrid strain analysis is proposed. In a special case with a built-up structure with unknown dynamic properties in the interfaces between the parts, the frequency- and spatial-dependent stress tensors, and thus also the traction vector, are obtained for the structural parts using the proposed technique.

The method is validated using numerical simulation of measured vibration responses, with very good agreement between the calculated and the true traction vector. The calculated traction vector is shown to converge towards the true traction vector in an arbitrary small area on the boundary of the structure.

The method is demonstrated for isotropic elastic material properties. This is, however, no limitation for the method; it can be also applied to a structure with anelastic material properties.

1. INTRODUCTION

In complex structures consisting of several structural parts, there are many sources of dissipation of vibration energy (damping) (see reference [1]). Probably, the most commonly known is material damping in anelastic materials. Another important source of damping in structures is the dissipation of vibration energy at interfaces (or joints) between structural parts, due to, for example, friction and air pumping [1]. Knowledge of the damping, both in the material and at interfaces between structural parts, is very important in built-up structures in order to predict the vibration field accurately. The estimation/modelling of damping at joints is an area that requires extensive research due to the small number of publication's available today. In order to describe the damping behaviour of the joints, it may be important to know the detailed dynamic traction vector acting on contact surfaces (or interfaces) between structural parts.

A hybrid technique for obtaining the detailed frequency and spatial dependent traction vector is proposed here. The method is an extension and application of the results reported by Sehlstedt [2], where a technique for obtaining dynamic strain tensor fields was presented. This technique, called hybrid strain analysis (HSA), is based on input from hybrid modal analysis (HMA). Hybrid modal analysis [3], is a method of obtaining the three-dimensional displacement field in a vibrating structure from a restricted set of measured vibration displacement response data combined with a set of elastic eigenmodes.

0022-460X/02/050921 + 17 $35.00/0

Based on the terminology used in the earlier methods, it is natural to denote the proposed method as hybrid traction analysis (HTA). Hybrid traction analysis should be interpreted as HSA applied to a built-up structure with unknown dynamic properties at the interfaces between the structural parts. The traction vector is then obtained at both the contact interfaces between different structural parts and within the structural parts. In the present application, it is assumed that the elastic and anelastic properties in the structural parts are known.

Normally, the traction vector is associated with the boundary surface traction vector, i.e., the traction vector acting on the boundary surface of the structure. It is important to note that the surface discussed here, in general, can be an internal one.

The problem of calculating the dynamic traction vector excitation acting on the boundary of a structure *from measured vibration responses* is usually referred to as the inverse problem. In several applications, when solving the inverse problem, it is often reported, (see for example references [4–10]) that the problem equations become ill-conditioned. In Sehlstedt [11], a well-conditioned technique for obtaining the spatial and frequency-dependent boundary traction vector is proposed. However, when using the method proposed here for obtaining the boundary traction vector, for example, at interfaces between structural parts, there is no problem with ill-conditioning; moreover, the dynamic stress tensor and needed traction vectors are obtained, not just on the boundary but, in the whole structure. In fact, the dynamic strain tensor is available at arbitrary points in the structure by means of HSA, and then the stress tensor and thus also the traction vector can be obtained at the same points from known material properties (both elastic and anelastic) of the structure in question.

Throughout the text the three-dimensional displacement field in the time domain is denoted by $\mathbf{u}(\mathbf{x}, t) \in \mathbb{R}^3$, and its frequency domain, Laplace transformed, counterpart is denoted with a *tilde* above the function, i.e., $\tilde{\mathbf{u}}(\mathbf{x}, s) \in \mathbb{C}^3$. Here, and in the following, $s = \alpha + \mathrm{i}\omega$ is a complex frequency variable where $\mathrm{i}(\mathrm{i}^2 = -1)$ denotes the imaginary unit and ω is the circular frequency (rad/s) of vibration; also, Hilbert space basis functions and elastic (normal) displacement (eigen) modes are used synonymously.

It is assumed here that any quasi-static contributions are neglected, i.e., the proposed method is only valid at frequencies higher than zero.

2. GOVERNING EQUATIONS

Consider a three-dimensional solid occupying a volume $\Omega \subset \mathbb{R}^3$. The motion of a vibrating body may be described by a time-dependent three-dimensional displacement field $\mathbf{u} = \mathbf{u}(\mathbf{x}, t)$ where $\mathbf{x}$ is a point in the body, and t is the time variable. If vanishing body forces are assumed, the time domain, matrix representation of (Cauchy's first) equations of motion are given by

$$-\mathbf{D}^{\mathrm{T}}[\boldsymbol{\sigma}] + \rho\ddot{\mathbf{u}} = \mathbf{0}, \tag{1}$$

where $\boldsymbol{\sigma} = \boldsymbol{\sigma}(\mathbf{x}, t)$ is the Voight-matrix representation of the symmetric Cauchy stress tensor, and $\mathbf{D}$ is a partial differential operator defined in Appendix A; the mass density distribution $\rho = \rho(\mathbf{x})$ is assumed to be time invariant.

The Laplace transformed, frequency domain (s-domain) counterpart to equation (1) can be stated as

$$-\mathbf{D}^{\mathrm{T}}[\tilde{\boldsymbol{\sigma}}] + s^2\rho\tilde{\mathbf{u}} = \mathbf{0}, \tag{2}$$

where $\tilde{\boldsymbol{\sigma}} = \tilde{\boldsymbol{\sigma}}(\mathbf{x}, s)$ and $\tilde{\mathbf{u}} = \tilde{\mathbf{u}}(\mathbf{x}, s)$ are the frequency domain stress and displacement fields respectively.

Following Dovstam [3], the stress–strain relationship for a linear non-hereditary material at isothermal conditions may be described by

$$\tilde{\boldsymbol{\sigma}} = \hat{\mathbf{H}}\tilde{\boldsymbol{\varepsilon}} = \hat{\mathbf{H}}\mathbf{D}[\tilde{\mathbf{u}}], \tag{3}$$

where $\hat{\mathbf{H}} = \hat{\mathbf{H}}(\mathbf{x}, s)$ is a complex, position- and frequency-dependent, constitutive 6×6 material matrix; and $\tilde{\boldsymbol{\varepsilon}} = \tilde{\boldsymbol{\varepsilon}}(\mathbf{x}, s)$ is the frequency domain strain field. Further, it is assumed that $\hat{\mathbf{H}}$ can be decomposed as

$$\hat{\mathbf{H}} = \mathbf{H} + \mathbf{H}_{\Delta}, \tag{4}$$

where $\mathbf{H}$ and $\mathbf{H}_{\Delta}$ denote the zero frequency, relaxed elastic properties, and the frequency-dependent anelastic properties respectively. Methods for estimating, $\mathbf{H}_{\Delta}$, for a specific isotropic material are described in Dovstam and Dalenbring [12] and Dalenbring [13].

The spatial and time-dependent Cauchy traction vector is defined as [14]

$$\mathbf{t}_n(\mathbf{x}, t) := \mathbf{N}\boldsymbol{\sigma}, \tag{5}$$

where the subscript n denotes the normal to the surface with Cartesian matrix representation $\mathbf{N}$ as defined in Appendix A. The Laplace transformed counterpart to equation (5) is defined as

$$\tilde{\mathbf{t}}_n(\mathbf{x}, s) := \mathbf{N}\tilde{\boldsymbol{\sigma}} = \mathbf{N}\hat{\mathbf{H}}\tilde{\boldsymbol{\varepsilon}}. \tag{6}$$

3. HYBRID RESPONSE MODEL

In this section the basic concepts of the hybrid response model used here, on which HMA and HSA are also based, will be briefly outlined. The term *hybrid* should be interpreted here as a mixture of measurements and continuous mode series expansion. For details of HMA and HSA see Dovstam [3] and Sehlstedt [2] respectively.

Here some important facts regarding Fourier series in Hilbert spaces will be emphasized when applied to three-dimensional functions and domains. In Appendix B, these facts will be discussed further.

Fourier series play an important role in the above-mentioned methods. The frequency domain Laplace transformed three-dimensional displacement field, $\tilde{\mathbf{u}} = \tilde{\mathbf{u}}(\mathbf{x}, s)$, may be represented by a generalized spatial Fourier series (or mode series expansion)

$$\tilde{\mathbf{u}}(\mathbf{x}, s) = \sum_{m=1}^{\infty} c_m(\tilde{\mathbf{u}})\,\mathbf{w}^{(m)}(\mathbf{x}), \tag{7}$$

where the s-dependent, i.e., frequency-dependent, coefficients $c_m(\tilde{\mathbf{u}})$ are linear functionals of the Laplace transformed displacement field, $\tilde{\mathbf{u}}$, defined in Appendix A; and the three-dimensional vector field $\mathbf{w}^{(m)} \in \mathbb{R}^3$, with real valued components, is the eigenmode number m with corresponding circular eigenfrequency ω_m satisfying a certain elastic eigenvalue problem (see Appendix B). The sequence $\{\mathbf{w}^{(m)}\}_{m=1}^{\infty}$ is referred to as a spatial Hilbert space basis, and it is thus complete. This will yield an $\mathbf{L}_2^3(\Omega)$-convergent series, i.e., convergent in the mean square sense (see Appendix B). The eigenmodes, $\mathbf{w}^{(m)}$, are assumed here to be dimensionless, and hence, the Fourier coefficients, $c_m(\tilde{\mathbf{u}})$, have the dimensions of length (m) if the modal masses, a_m defined in Appendix A, have dimensions of weight (kg).

The HMA technique for obtaining the three-dimensional displacement field is essentially a method for estimating the Fourier coefficients, $c_m(\tilde{\mathbf{u}})$. By means of measured vibration responses (displacement, or velocity/acceleration transformed into displacement) and numerical approximations (e.g. using the finite element method (FEM)) to the eigenmodes, $\mathbf{w}^{(m)}$, the Fourier coefficients, $c_m(\tilde{\mathbf{u}})$, are obtained by a least-squares fit. Based on a truncated version of equation (7), least-squares estimates for the Fourier coefficients can be obtained as outlined below.

Assume that up to M number of modes are to be used in the truncated version of the infinite mode series expansion (7). Then, for the measured displacement response, $\tilde{U}_i^{mea}$, at a point $p(i)$ with co-ordinate $\mathbf{x}_{p(i)}$ and measurement direction $\hat{\mathbf{n}}_i$ ($\hat{\mathbf{n}}_i$ being a three-dimensional vector of unit length), the following relationship is obtained:

$$\tilde{\mathbf{U}}^{mea} = \mathbf{A}\tilde{\mathbf{C}} + \tilde{\mathbf{U}}^{res}, \tag{8}$$

where $\mathbf{A}$ is a real and constant $N \times M$ response matrix (N being the number of measured responses), with components defined as $A_{im} := \hat{\mathbf{n}}_i \cdot \mathbf{w}^{(m)}(\mathbf{x}_{p(i)})$, relating the Fourier coefficients, arranged in the vector $\tilde{\mathbf{C}}$, to the displacements; the vector $\tilde{\mathbf{C}}$ is defined such that

$$\tilde{\mathbf{C}} := [c_1(\tilde{\mathbf{u}}), c_2(\tilde{\mathbf{u}}), \ldots, c_M(\tilde{\mathbf{u}})]^{\mathrm{T}}. \tag{9}$$

Note that at each point $p(i)$ there can be up to three responses, $\tilde{U}_i^{mea}$, i.e., if measurements are performed in more than one direction at $p(i)$; this means that $p(i) = p(j)$, for $i \neq j$ is possible. Thus, the set of measurement points is $p \in \{1, \ldots, P\}$, such that $P \leqslant N$.

Finally, $\tilde{\mathbf{U}}^{res}$ in equation (8) is the residual caused by truncation of the infinite series as in equation (7). Approximation of the residual and the consequence of neglecting the residual were discussed in Dovstam [3] and Sehlstedt [2].

If the residual is neglected a higher number of modes have to be used, M, in the truncated version of the mode series expansion (7); this implies a higher number of measurements, N, in order to resolve the eigenmode with shortest wavelength used in the (mode) series expansion (7).

Now least-squares estimates of the Fourier coefficients, $c_m(\tilde{\mathbf{u}})$, can be obtained by means of equation (8), i.e., $\tilde{\mathbf{C}}$ can be estimated as

$$\tilde{\mathbf{C}} = \mathbf{A}^{+}(\tilde{\mathbf{U}}^{mea} - \tilde{\mathbf{U}}^{res}), \tag{10}$$

where $\mathbf{A}^{+}$ is the pseudo-inverse of $\mathbf{A}$.

Knowing the coefficients, $c_m(\tilde{\mathbf{u}})$, $m \in \{1, \ldots, M\}$, displacement response can be predicted at arbitrary points in the vibrating structure by means of the eigenmode fields $\mathbf{w}^{(m)} = \mathbf{w}^{(m)}(\mathbf{x})$, $m \in \{1, \ldots, M\}$, the series expansion, and possibly some approximation to the residual $\tilde{\mathbf{U}}^{res}$. Then by means of numerical differentiation, the dynamic strain tensor field is obtained using the predicted displacement field and the definition of the strain tensor (A6).

Of course, $N \geqslant M$ and it should be stressed that the measurements must be carried out so that they can resolve the shortest wavelength of the eigenmodes, $\mathbf{w}^{(m)}$, used which is influenced by the characteristics of the vibration field, $\tilde{\mathbf{u}}$.

4. DYNAMIC TRACTION VECTOR ESTIMATION

In a complex structure consisting of several structural parts with interfaces (or joints) between the parts, there is often no knowledge of the dynamic properties of the interface, i.e.,

no physical model exists describing the dissipation of vibration energy (damping) at the interface. As mentioned in section 1, this damping behaviour is due to, for example, friction and air pumping.

Accurate knowledge of the traction vector field is a good starting point for deriving physical models describing this kind of damping. One of the objectives for the proposed method is the accurate description of the frequency and spatial-dependent traction vector acting on the interfaces between structural parts.

Now by applying the hybrid strain response model from section 3, the dynamic strain tensor *field* for the (whole) body Ω can be predicted. Then the dynamic traction vector *field* can be obtained by means of the definition; that is, equation (6) and known elastic and anelastic properties, (equations (3) and (4)), of the structure in question. This is a straightforward task; but there are some aspects regarding the eigenmodes when using the HTA method proposed below that need to be addressed.

The lack of knowledge about the dynamic properties of the interfaces is, in the proposed method, overcome by assuming some *fictitious* but appropriate geometrical extension, elastic properties and mass distribution for the interfaces and including them and the structural parts in a volume, Ω_w, such that $\Omega_w := \Omega \cup \Omega_{fict}$, where Ω_{fict} denotes the volume of the fictitious part consisting of the fictitious geometrical extension of the interfaces. Note that the contact area can always be assumed to be known, and hence the fictitious extension will only be in one direction. Then by solving the elastic eigenvalue problem, as in equations (B.1) and (B.2) (with Ω_w as the body), elastic eigenmodes describing some "movement" between structural parts at the interfaces can be obtained. In practice (and in theory), one will find different properties in Ω and in the fictitious part Ω_{fict}. However, the "true" properties of the fictitious part, Ω_{fict}, need not be known. The only requirement for the eigenmodes obtained is to span the Hilbert space $\mathbf{L}_2^3(\Omega_w)$ and approximate the displacement field, $\tilde{\mathbf{u}}$, in the body Ω accurately enough, with as low a number of eigenmodes as possible.

The question is what kind of geometrical extension, elastic properties and mass distribution should be assumed for the fictitious part, Ω_{fict}. There is no unique answer to this question; but in practice, the choice is guided by minimizing the error between predicted displacement responses and separately measured displacement spectra not used in the estimation of the Fourier coefficient spectra. It must be kept in mind that only a limited number of eigenmodes is needed, which is computationally inexpensive to obtain. Therefore, even if the eigenvalue problem needs to be solved several times, in order to obtain the best choice for the properties in the fictitious part, Ω_{fict}, it will not make the proposed method computationally demanding. Also, it must be kept in mind that the proposed method is intended as a tool for the estimation/modelling of damping at interfaces between structural parts, and hence the issue of computer time is not the most important.

The proposed technique, HTA, can be summarized as follows:

(1) Measure N number of vibration responses at a number of points on the structure. The number N should be chosen to be large enough compared with the number of needed modes, M, so that the system of equations, as in equation (8), is sufficiently over-determined, and such that the shortest wavelength of the eigenmodes, $\mathbf{w}^{(m)}$, used in the series expansion can be resolved, which is influenced by the wavelengths of the vibration field, $\tilde{\mathbf{u}}$. Note that at some of the measurement points, measurements in all three Cartesian directions are needed in order to resolve the motion;

(2) Assume some initial values for the geometrical extension, elastic properties and mass distribution for the fictitious part, Ω_{fict}, and solve the elastic eigenvalue problem for the whole structure, Ω_w, i.e., as in equations (B.1) and (B.2), with a detailed geometrical

description, i.e., a sufficiently high number of finite elements if the generation of the $\mathbf{w}^{(m)}$-basis is based on the FEM;

(3) Residual approximation, if the excitation is known. If the number of modes, M, is high enough the residual can be neglected. Note that the residual approximation can actually worsen the results. An indication of this will be noticed when validating the coefficient spectra, as in item **5**;

(4) Fourier coefficient spectra estimation, using equation (10);

(5) Validation of coefficient spectra using the truncated version of equations (7), and measured validation spectra not used in the estimation of the Fourier coefficient spectra, as in item 4;

(6) Assume new values for the properties for the fictitious part, Ω_{fict}, and carry out 2–5 until the convergence criterion is fulfilled, i.e., the error between the predicted and separately measured validation spectra is minimized;

(7) Displacement response prediction at $3n + 1$ points, i.e., the point of interest and n adjacent points in each (Cartesian) co-ordinate direction, using the truncated version of equation (7);

(8) Strain tensor calculation using finite difference schemes of order n and equation (A.6). It is assumed that the numerical differentiation is performed by $n + 1$ point finite difference schemes (see reference [2]);

(9) Traction vector estimation using the calculated strain tensor and equation (6).

It is important to emphasize that the geometrical extension, elastic properties and mass distribution of the fictitious part, Ω_{fict}, only have to be chosen so as to yield a low error between separately measured validation spectra and their corresponding simulations based on equation (7). Note that the true material properties have to be known for the body, Ω, under study.

Note also that, by means of the method proposed above, the dynamic stress tensor, and thus also the traction vector, is obtained (within the actual limits of displacement wavelengths and maximum frequency of vibration) at *any* point in the structure, not just at the interface between the structural parts.

5. NUMERICAL TEST CASE

The method proposed in section 4 will be validated numerically in this section by means of the FEM, i.e., the necessary measured responses are simulated using FEM. The test structure is the same as in [11], i.e., an aluminium plate having dimensions $0{\cdot}520 \times 0{\cdot}300 \times 0{\cdot}0042\,\text{m}$ $(x \times y \times z)$. The plate is attached to two supports consisting of Plexiglas (PMMA) and having dimensions $0{\cdot}01 \times 0{\cdot}300 \times 0{\cdot}01$ m $(x \times y \times z)$, as depicted in Figure 1. The two supports are modelled as attached to the plate along one edge ($z = 0{\cdot}0\,\text{m}$)

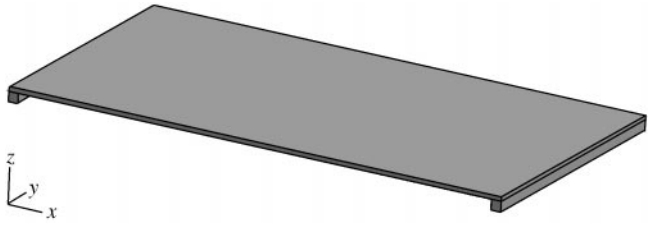

Figure 1. The test structure.

and fixed to the ground along the other edge ($z = -0{\cdot}01$ m). The supports simulate some true interfaces between the plate and the ground. The objective is to calculate the traction vector field at the interfaces using only the information of the contact area as *a prior* knowledge for the supports.

The elastic material properties for the aluminium plate are $\rho_{Al} = 2795$ kg/m^3 for the mass density distribution, and zero frequency Young's modulus and the Poisson ratio $E_{Al} = 73{\cdot}0$ GPa and $\nu_{Al} = 0{\cdot}3260$, respectively; and for the Plexiglas supports $\rho_{PMMA} = 1181$ kg/m^3, $E_{PMMA} = 3{\cdot}44$ GPa and $\nu_{PMMA} = 0{\cdot}3820$. The anelastic properties of the Plexiglas are neglected for simplicity; note that this is no restriction for the proposed method.

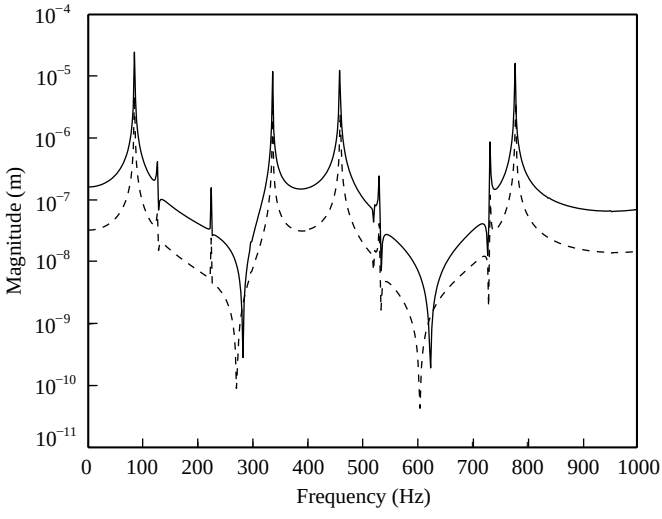

Figure 2. Initial simulation of independent displacement response in the x direction: ——, direct FE-calculated; - - -, simulated.

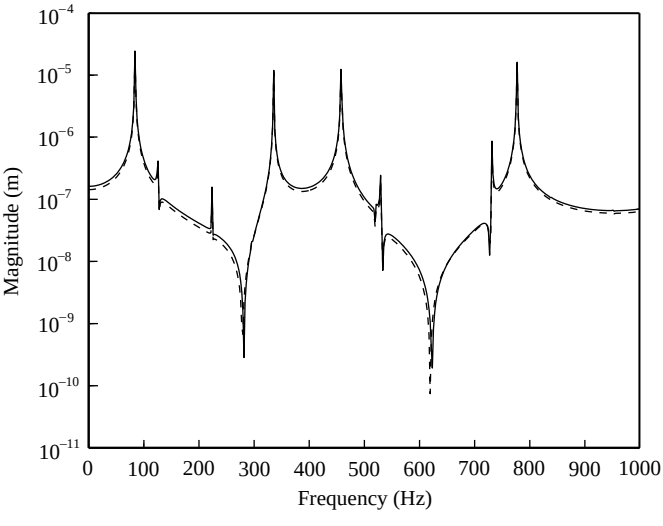

Figure 3. Final validation of independent displacement response in the x direction: ——, direct FE-calculated; - - -, simulated.

Numerical simulation of *measured* responses ($\tilde{\mathbf{U}}^{mea}$ in equation (8)) is obtained by direct finite element (FE) calculations in MSC Nastran™ resulting in a discrete finite dimensional response model [3], with a total number of 94 "measurement" points with displacement, in all three (Cartesian) directions. The residual, $\tilde{\mathbf{U}}^{res}$, in equation (8) is neglected completely.

The FE mesh for the plate consists of 18 720 (solid) elements, with eight grid points in each element. The total number of grid points is 25 620, with four grid points, i.e., three elements, through the thickness. For the Plexiglas supports these numbers are: 1440 solid elements with a total of 2562 grid points. This gives a grand total of 27 816 grid points and 20 160 elements for the complete structure (the plate and supports). The plate is excited by a traction vector, $\tilde{\mathbf{t}}_n = [1, 9, 9]^{\mathrm{T}}$ Pa, acting at a point with location $\mathbf{x}_e = [0{\cdot}2600, 0{\cdot}1600, 0{\cdot}0042]^{\mathrm{T}}$ m.

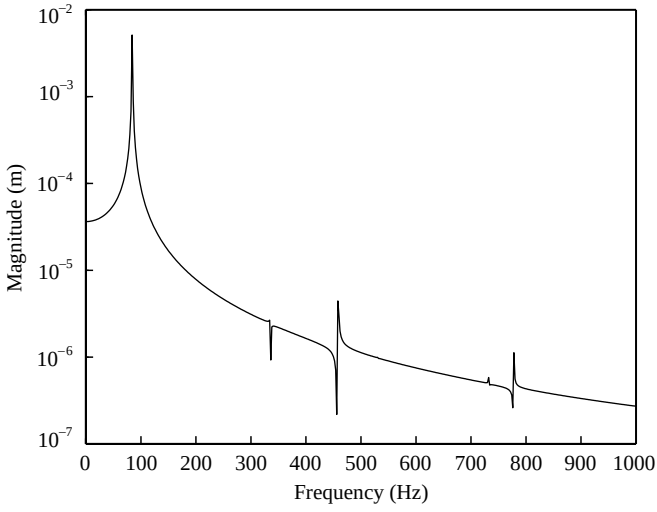

Figure 4. Fourier coefficient for $m = 1$, i.e., $c_1(\tilde{\mathbf{u}})$.

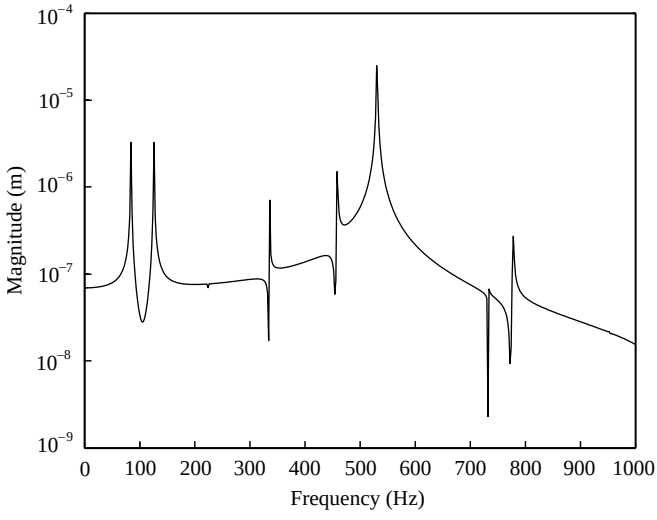

Figure 5. Fourier coefficient for $m = 8$, i.e., $c_8(\tilde{\mathbf{u}})$.

Following the discussion in section 4 about fictitious geometrical extension and material properties for the interfaces, that is, in this case the supports, some initial values are assumed. The elastic eigenvalue problem is then solved by means of MSC Nastran™ for the structure including the plate and the fictitious extension, i.e., $\Omega_w = \Omega \cup \Omega_{fict}$. As a first guess the elastic eigenvalue problem is solved using the assumption that Ω_w consists of aluminium, and has geometrical extension in the negative z direction of 0·005 m for both fictitious extensions. The dimensions in the x and y directions are of course known since the contact surface can always assumed to be known. Then validation, by equation (10), of the calculated Fourier coefficients with independently FE-calculated displacement spectra is performed. One example of this validation can be seen in Figure 2. A total number of 100

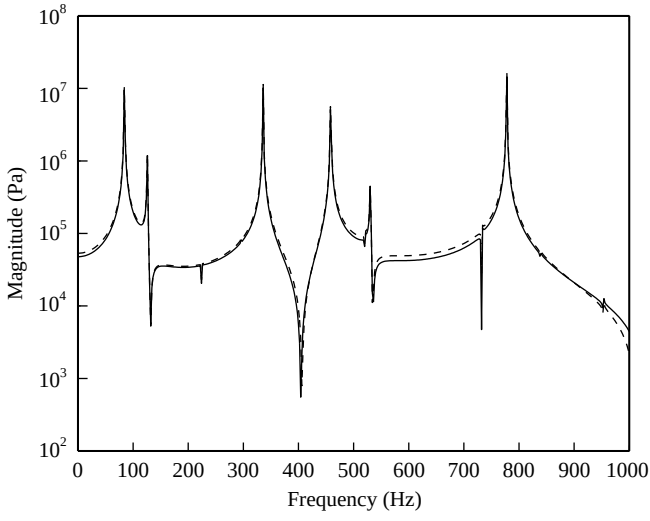

Figure 6. HTA calculated traction vector compared with the true traction vector, in the x direction, at $\mathbf{x} = [0{\cdot}01, 0{\cdot}005, 0{\cdot}00]^{\mathrm{T}}$: ——, true; - - -, HTA calculated.

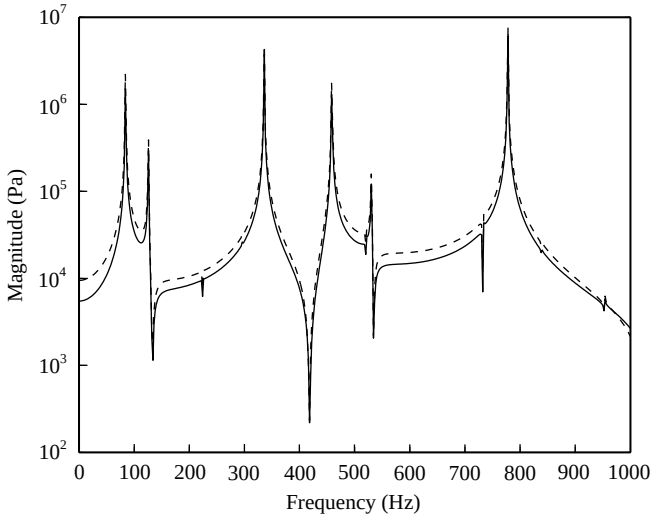

Figure 7. HTA calculated traction vector compared with the true traction vector, in the y direction, at $\mathbf{x} = [0{\cdot}01, 0{\cdot}005, 0{\cdot}00]^{\mathrm{T}}$: ——, true; - - -, HTA calculated.

modes are used in the mode series expansion, i.e., 100 Fourier coefficients were calculated using equation (10). As can be seen in Figure 2, the predicted displacement is slightly lower than the true one; therefore, one can conclude that the stiffnesses in the fictitious extensions, Ω_{fict}, are a little too high. A second eigenmode calculation using $E_{support} = 5$ GPa for the fictitious extensions, but otherwise the same material properties as for aluminium and the same geometrical extension as before, gave a very good simulation of the displacement in the aluminium plate as can be seen in Figure 3. Here, as before, 100 modes were calculated.

It cannot be overemphasized that the *only* role for the eigenmodes is to span $\mathbf{L}_2^3(\Omega_w)$ and approximate the displacement field sufficiently accurately using the lowest possible number of eigenmodes. Here $\mathbf{L}_2^3(\Omega_w)$ is the space of square integrable, three-dimensional continuous functions in Ω_w.

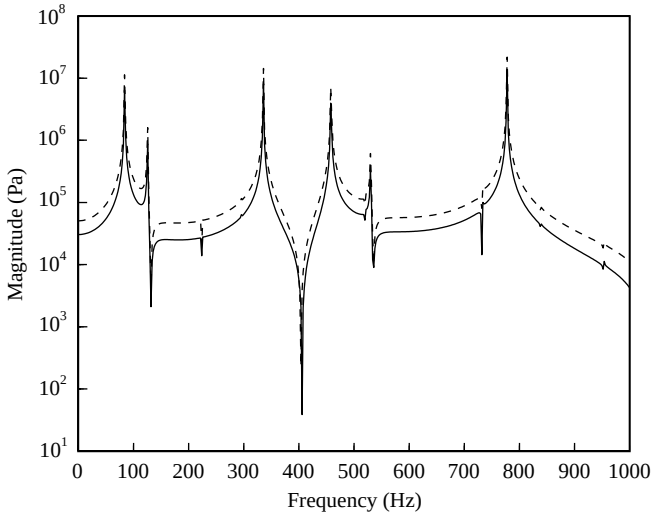

Figure 8. HTA calculated traction vector compared with the true traction vector, in the z direction, at $\mathbf{x} = [0{\cdot}01, 0{\cdot}005, 0{\cdot}00]^{\mathrm{T}}$: ——, true; - - -, HTA calculated.

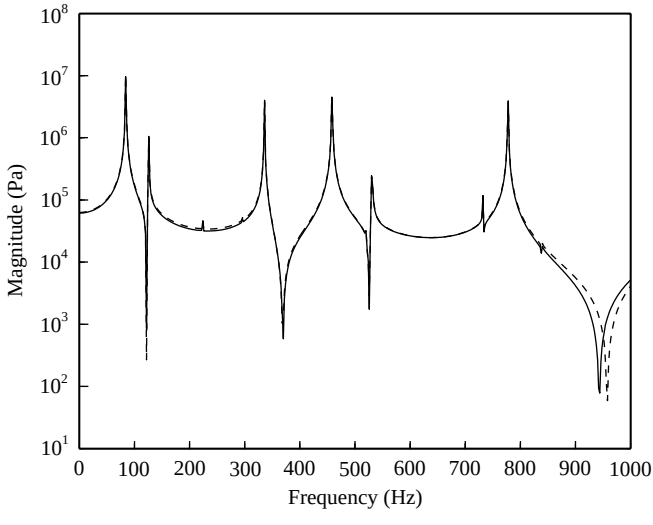

Figure 9. HTA calculated traction vector compared with the true traction vector, in the x direction, at $\mathbf{x} = [0{\cdot}51, 0{\cdot}26, 0{\cdot}00]^{\mathrm{T}}$: ——, true; - - -, HTA calculated.

In Figures 4 and 5, the estimated Fourier coefficients for modes number 1 and 8, i.e., $c_1(\tilde{\mathbf{u}})$ and $c_8(\tilde{\mathbf{u}})$ are depicted. It can be seen that each Fourier coefficient has more than one peak. This is due to the fact that the Fourier coefficients are coupled to each other, i.e., $c_m(\tilde{\mathbf{u}})$ and $c_r(\tilde{\mathbf{u}})$, $m \neq r$, depend on each other. Here the coupling is due to the fact that the eigenmodes that span $\mathbf{L}_2^3(\Omega_w)$ are used to simulate response in a body which is different from Ω_w.

The traction vector calculated by means of HTA is compared with the true traction vector. The true traction vector is obtained using definition (6) and direct FE computed displacements. The spatial derivatives in equation (6) are calculated using numerical differentiation, in three point non-equidistant finite difference schemes (see reference [2]).

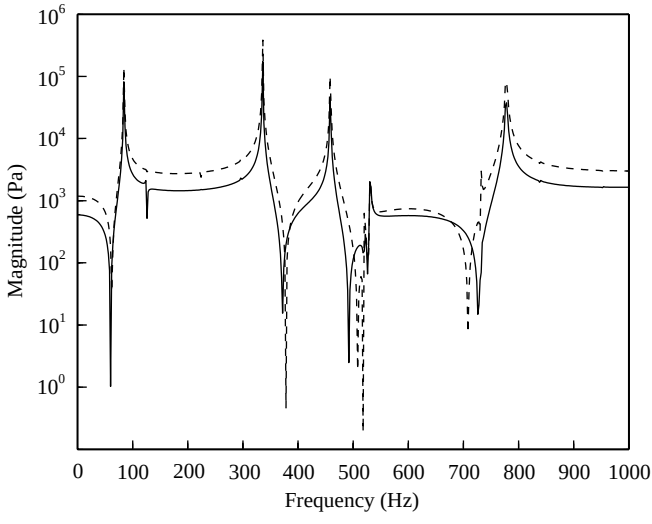

Figure 10. HTA calculated traction vector compared with the true traction vector, in the y direction, at $\mathbf{x} = [0{\cdot}51, 0{\cdot}26, 0{\cdot}00]^{\mathrm{T}}$: ——, true; - - -, HTA calculated.

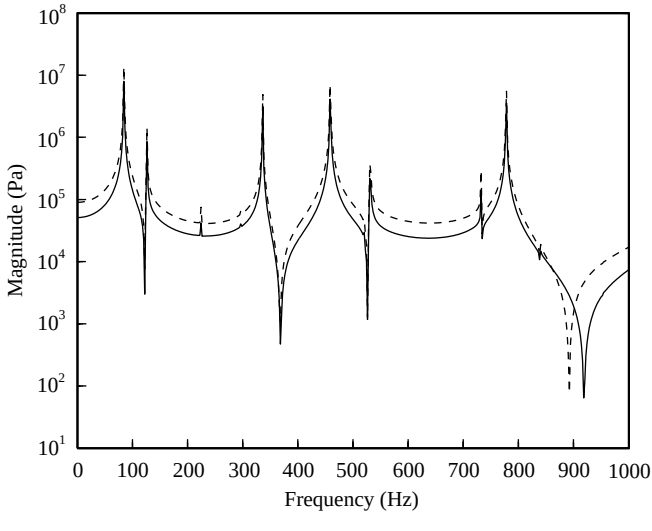

Figure 11. HTA calculated traction vector compared with the true traction vector, in the z direction, at $\mathbf{x} = [0{\cdot}51, 0{\cdot}26, 0{\cdot}00]^{\mathrm{T}}$: ——, true; - - -, HTA calculated.

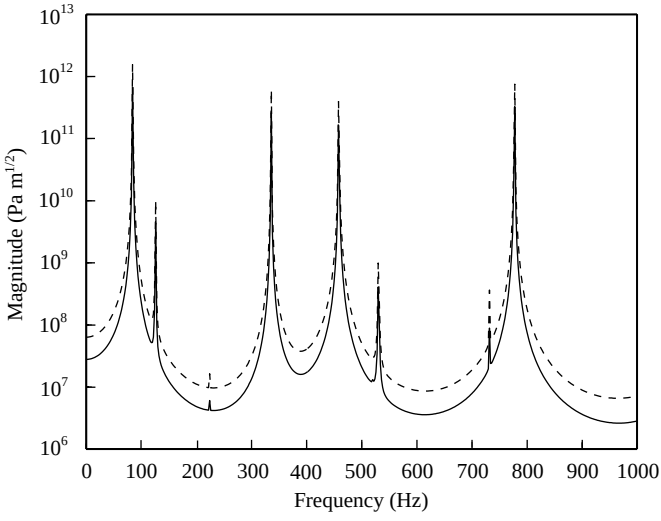

Figure 12. Boundary norm of HTA calculated traction vector compared with boundary norm of the true traction vector: ——, true; - - -, HTA calculated.

Also in HTA three point non-equidistant finite difference schemes are used. This comparison can be seen in Figures 6–11 for two different points at the interfaces between the plate and the supports. Apart from a few exceptions the agreement is very good.

Note that the stress tensor can be estimated in all 25 620 grid points in the FE-model of the plate, making a total of $25\,620 \times 6 = 153\,720$ stress tensor components using only $94 \times 3 = 282$ displacement components in the proposed method. Thereafter, the traction vector can be obtained at the desired surface for each of the 25 620 grid points.

The norm for a three-dimensional vector field on the boundary, $\|\cdot\|_{\mathbf{L}_2^3(\partial\Omega)}$, as defined in Appendix A, is calculated for the HTA-calculated and true traction vector and the results are depicted in Figure 12, where it can be seen that the agreement is good.

6. SUMMARY AND DISCUSSION

In this paper, a method denoted as hybrid traction analysis (HTA), for the estimation of the dynamic traction vector is proposed. The method is based on hybrid strain analysis where a restricted number of measured vibration responses and approximations to a spatial Hilbert space basis combined with numerical differentiation yield the dynamic strain tensor field. Hybrid traction analysis is an extension and special application of hybrid strain analysis to the case of a built-up structure with unknown dynamic properties in the interfaces between the structural parts. The dynamic stress tensor and thus also the traction vector is obtained not just at the interfaces but in the whole structure in question, since the elastic and anelastic material properties of the structure is assumed to be known.

It is emphasized that the displacement measurements must be carried out in all three Cartesian directions, e.g., by means of triaxial accelerometers, at least for a subset of the set of measurement points.

Together with the method presented in reference [11] the method proposed here may be used as a tool for calculating the dynamic boundary traction vector acting on, for example, interfaces between structural parts. This is a good starting point for deriving physical models describing damping at joints and interfaces between different parts.

ACKNOWLEDGMENTS

This work was performed under contract from the Swedish Defence Material Administration (FMV). The funding provided is gratefully acknowledged. The author would like to thank all staff of the Structural Dynamics research group, Department of Structures and Materials, Aeronautics Division, Swedish Defence Research Agency.

REFERENCES

1. A. D. NASHIF, D. I. JONES and J. P. HENDERSON 1985 *Vibration Damping*. New York: John Wiley & Sons, Inc.
2. N. SEHLSTEDT 2001 *Journal of Sound and Vibration* **244**, 407–430. Calculating the dynamic strain tensor field using modal analysis and numerical differentiation.
3. K. DOVSTAM 1998 *Computational Mechanics* **21**, 493–511. Real modes of vibration and hybrid modal analysis.
4. B. J. DOBSON and E. RIDER 1990 *Proceedings of the Institution of Mechanical Engineers* **204**, 69–75. A review of the indirect calculation of excitation forces from measured structural response data.
5. J. M. STARKEY and G. L. MERRILL 1989 *International Journal of Analytical and Experimental Modal Analysis* **4**, 103–108. On the ill-conditioned nature of indirect force-measurement techniques.
6. M. HANSEN and J. M. STARKEY 1990 *Proceedings of the* 8*th IMAC*, 115–120. On predicting and improving the condition of modal-model-based indirect force measurement algorithms.
7. J. D'CRUZ, J. D. C. CRISP and T. G. RYALL 1992 *Journal of Applied Mechanics* **59**, 722–729. On the force identification of harmonic force on a viscoelastic plate from response data.
8. J. F. DOYLE 1993 *Experimental Mechanics* **33**, 64–69. Force identification from dynamic responses of a bimaterial beam.
9. F. D. BARTLETT JR and W. G. FLANNELLY 1979 *Journal of American Helicopter Society* **24**, 10–18. Model verification of force determination for measuring vibratory loads.
10. P. W. MÖLLER 1999 *Journal of Applied Mechanics* **66**, 236–241. Load identification through structural modification.
11. N. SEHLSTEDT 2001 *Computational Mechanics*, accepted for publication. A well-conditioned technique solving the inverse problem of boundary traction estimation for a constrained vibrating structure.
12. K. DOVSTAM and M. DALENBRING 1997 *Computational Mechanics* **19**, 271–286. Damping function estimation based on modal receptance models and neural nets.
13. M. DALENBRING 1999 *Mechanical Systems and Signal Processing* **13**, 547–569. Damping function estimation based on measured vibration frequency responses and finite-element displacement modes.
14. G. A. HOLZAPFEL 2000 *Nonlinear solid mechanics*. West Sussex: John Wiley & Sons Inc.
15. R. D. RICHTMYER 1978 *Principles of Advanced Mathematical Physics*, Vol. 1. New York: Springer-Verlag.
16. M. E. GURTIN 1972 in *The Linear Theory of Elasticity*, *Encyclopedia of Physics*, *Volume* VI*a*/2, *Mechanics of Solids* II (S. Flügge and C. Trusdell, editors). Berlin: Springer-Verlag.
17. D. REDDY 1997 *Introductory Functional Analysis*. New York: Springer-Verlag.

APPENDIX A: DEFINITIONS

The displacement field, $\mathbf{u}$, the Voight-matrix representation of the symmetric stress tensor field, $\boldsymbol{\sigma}$, and strain tensor field, $\boldsymbol{\varepsilon}$, in Cartesian co-ordinates are defined as

$$\mathbf{u} := \mathbf{u}(\mathbf{x},\ t) = [u_1\ u_2\ u_3]^{\mathrm{T}}, \tag{A.1}$$

$$\boldsymbol{\sigma} := \boldsymbol{\sigma}(\mathbf{x}, t) = [\sigma_{11}\ \sigma_{22}\ \sigma_{33}\ \sigma_{12}\ \sigma_{23}\ \sigma_{31}]^{\mathrm{T}} \tag{A.2}$$

$$\boldsymbol{\varepsilon} := \boldsymbol{\varepsilon}(\mathbf{x}, t) = [\varepsilon_{11}\ \varepsilon_{22}\ \varepsilon_{33}\ \ 2\varepsilon_{12}\ 2\varepsilon_{23}\ 2\varepsilon_{31}]^{\mathrm{T}}, \tag{A.3}$$

where $\mathbf{x} = [x_1, x_2, x_3]^{\mathrm{T}}$ and t is the time variable.

The linear strain–displacement field relations are given as

$$\varepsilon_{ik} = \frac{1}{2}\left[\frac{\partial u_i}{\partial x_k} + \frac{\partial u_k}{\partial x_i}\right]. \tag{A.4}$$

Thus the first order (strain), partial differential operator matrix can be defined as

$$\mathbf{D} := \begin{bmatrix} \dfrac{\partial}{\partial x_1} & 0 & 0 \\ 0 & \dfrac{\partial}{\partial x_2} & 0 \\ 0 & 0 & \dfrac{\partial}{\partial x_3} \\ \dfrac{\partial}{\partial x_2} & \dfrac{\partial}{\partial x_1} & 0 \\ 0 & \dfrac{\partial}{\partial x_3} & \dfrac{\partial}{\partial x_2} \\ \dfrac{\partial}{\partial x_3} & 0 & \dfrac{\partial}{\partial x_1} \end{bmatrix}, \tag{A.5}$$

so that the strain field can be expressed as

$$\boldsymbol{\varepsilon} = \mathbf{D}\,[\mathbf{u}]. \tag{A.6}$$

The Cartesian matrix representation, $\mathbf{N} = \mathbf{N}(\mathbf{x})$, of the unit normal vector field, $\mathbf{n}(\mathbf{x}) = [n_1, n_2, n_3]^{\mathrm{T}}$, is defined as

$$\mathbf{N} := \begin{bmatrix} n_1 & 0 & 0 & n_2 & 0 & n_3 \\ 0 & n_2 & 0 & n_1 & n_3 & 0 \\ 0 & 0 & n_3 & 0 & n_2 & n_1 \end{bmatrix}. \tag{A.7}$$

The $\mathbf{L}_2^3(\Omega) = \mathrm{L}_2(\Omega) \times \mathrm{L}_2(\Omega) \times \mathrm{L}_2(\Omega)$ inner product $(\mathbf{u}, \mathbf{v})$ on the domain $\Omega \subset \mathbb{R}^3$ is defined as (see reference [15])

$$(\mathbf{u}, \mathbf{v}) := \int_\Omega \mathbf{u} \cdot \mathbf{v}^* \, \mathrm{d}\Omega = \int_\Omega (u_1 v_1^* + u_2 v_2^* + u_3 v_3^*) \, \mathrm{d}\Omega, \tag{A.8}$$

where $\mathbf{u}$ and $\mathbf{v}$ are some continuous functions, and $\mathbf{v}^*$ denotes the complex conjugate of the three-dimensional vector field $\mathbf{v}$. The inner product for vector fields on the boundary, $\partial\Omega$, is defined as

$$(\mathbf{u}, \mathbf{v})_{\partial\Omega} := \int_{\partial\Omega} \mathbf{u} \cdot \mathbf{v}^* \, \mathrm{d}\partial\Omega. \tag{A.9}$$

The natural norm in $\mathbf{L}_2^3(\Omega)$ is then defined as

$$\|\mathbf{u}\|_{\mathbf{L}_2^3(\Omega)} := \sqrt{(\mathbf{u}, \mathbf{u})} = \sqrt{\int_\Omega |\mathbf{u}|^2 \, \mathrm{d}\Omega}. \tag{A.10}$$

The $\mathbf{L}_2^3(\partial\Omega)$ norm for $\mathbf{u} \in \mathbb{C}^3$ on the boundary $\partial\Omega$ is defined as

$$\|\mathbf{u}\|_{\mathbf{L}_2^3(\partial\Omega)} := \sqrt{(\mathbf{u}, \mathbf{u})_{\partial\Omega}} = \sqrt{\int_{\partial\Omega} |\mathbf{u}|^2 \, \mathrm{d}\partial\Omega}. \tag{A.11}$$

The Fourier coefficients for the series expansion of the displacement field are defined as

$$c_m(\tilde{\mathbf{u}}) := \frac{(\tilde{\mathbf{u}}, \rho \mathbf{w}^{(\mathrm{m})})}{a_m}, \tag{A.12}$$

$$a_m := (\mathbf{w}^{(m)}, \rho \mathbf{w}^{(m)}) > 0, \tag{A.13}$$

where a_m are the modal masses.

For two six-dimensional vector fields, $\mathbf{E}$ and $\mathbf{V}$, the $\mathbf{L}_2^6(\Omega)$ inner product is denoted as $\langle \mathbf{E}, \mathbf{V} \rangle$ and defined analogous to the above.

The l_2-norm for an n-dimensional, real or complex, vector $\mathbf{y} = [y_1, y_2, \ldots, y_n]$ is defined as

$$|\mathbf{y}| := \sqrt{\sum_{i=1}^{n} |y_i|^2}. \tag{A.14}$$

when $\mathbf{y}$ is a real vector, the above norm is the well-known Euclidean norm.

The isotropic, elastic generalized Hooke's law relating the elastic stress vector with the strain vector can be expressed as

$$\mathbf{H} = \lambda \cdot \mathbf{H}_\lambda + G \cdot \mathbf{H}_G, \tag{A.15}$$

where $\lambda = 2\nu \cdot G/(1 - 2\nu)$, $G = E/(2(1 + \nu))$, $(\mathbf{H}_\lambda)_{ik} = 1$ for $i, k \leqslant 3$, and $(\mathbf{H}_G)_{ii} = 2$ for $i \leqslant 3$ and $(\mathbf{H}_G)_{ii} = 1$ for $4 \leqslant i \leqslant 6$.

APPENDIX B: FOURIER SERIES IN THE HILBERT SPACE $\mathbf{L}_2^3(\Omega)$

Let Ω be a compact (i.e., closed and bounded) set as defined in section 2, such that $\Omega \subset \mathbb{R}^3$; also, let $\mathbf{L}_2^3(\Omega)$ be a Hilbert space with metric $d(\mathbf{u}, \mathbf{v}) := \|\mathbf{u} - \mathbf{v}\|_{\mathbf{L}_2^3(\Omega)}$, where $\|\cdot\|_{\mathbf{L}_2^3(\Omega)}$ is the $\mathbf{L}_2^3(\Omega)$-norm defined in Appendix A, and $\mathbf{u}$ and $\mathbf{v}$ are some continuous (three-dimensional) functions. Note that $\mathbf{L}_2^3(\Omega) := \mathrm{L}_2(\Omega) \times \mathrm{L}_2(\Omega) \times \mathrm{L}_2(\Omega)$, where $\mathrm{L}_2(\Omega)$ is the usual Hilbert space of square integrable scalar (complex) valued functions, i.e., $\mathbf{L}_2^3(\Omega)$ is the space of square integrable three-dimensional vector valued functions. Recall that a Hilbert space is a complete inner product space, and an inner product space is a vector space with an inner product. Completeness means that every Cauchy sequence converges. Here the inner product is denoted by $(\cdot, \cdot)$ and defined in Appendix A.

Let the three-dimensional real valued vector field $\mathbf{w}^{(m)} = [w_1^{(m)}, w_2^{(m)}, w_3^{(m)}]^{\mathrm{T}} \in \mathbb{R}^3$ be the mode shape number m with corresponding circular eigenfrequency ω_m, i.e., $\mathbf{w}^{(m)}$ is assumed to be the eigenpair to an elastic eigenvalue problem with equations of motion

$$-\mathbf{D}^{\mathrm{T}}\mathbf{H}\mathbf{D}[\mathbf{w}^{(m)}] = \omega_m^2 \rho \mathbf{w}^{(m)} \tag{B.1}$$

and homogeneous Neumann and Dirichlet boundary conditions fulfilling

$$(\mathbf{N}\mathbf{H}\mathbf{D}[\mathbf{w}^{(m)}], \mathbf{w}^{(r)})_{\partial\Omega} = 0 \quad \forall m, r. \tag{B.2}$$

Then it is guaranteed that the continuous (real) modes of vibration, $\{\mathbf{w}^{(m)}\}_{m=1}^{\infty}$, constitute a set of complete basis functions in the Hilbert space $\mathbf{L}_2^3(\Omega)$, (see Gurtin [16]), where it was proved for a material continuous body). It is assumed here to be also valid for a material discontinuous body. In addition to completeness, the modes are orthogonal

$$(\mathbf{w}^{(m)}, \rho \mathbf{w}^{(r)}) = a_m \delta_{mr} \quad \forall m, r, \tag{B.3}$$

where δ_{mr} is the Kronecker delta, and a_m are the modal masses as defined in Appendix A.

Now, due to the completeness, it can be shown (see Reference [17]) that

$$\lim_{M \to \infty} \left\| \sum_{m=1}^{M} c_m(\tilde{\mathbf{u}})\, \mathbf{w}^{(m)} - \tilde{\mathbf{u}} \right\|_{\mathbf{L}_2^3(\Omega)} = 0, \tag{B.4}$$

where $c_m(\tilde{\mathbf{u}})$, $m \in [1, \infty]$, are the Fourier coefficients as defined in Appendix A and obtained using the concepts of HMA, as summarized in section 3. Further, the best approximation theorem (reference [17]), states that the Fourier coefficients as defined in Appendix A are the coefficients that provide the best approximation.

APPENDIX C: NOMENCLATURE

$\mathbf{A}$	modal response matrix
a_m	modal mass number m
$\mathbb{C}^3$	three-dimensional complex space
$\tilde{\mathbf{C}}$	vector of estimated Fourier coefficients
$c_m(\tilde{\mathbf{u}})$	Fourier coefficient number m
$\mathbf{D}$	strain operator matrix
E	Young's modulus
$\hat{\mathbf{H}}$	complex, position and frequency-dependent material matrix
$\mathbf{H}$	elastic generalized Hooke's matrix
$\mathbf{H}_{\Delta}$	position and frequency-dependent anelastic material properties
$\mathrm{L}_2(\Omega)$	Hilbert space of square integrable functions
$\mathbf{L}_2^3(\Omega)$	Hilbert space of square integrable three-dimensional vector valued functions
G	shear modulus
M	number of modes used in series expansion of the displacement field
$\mathbf{N}$	matrix representation of the unit normal vector
N	number of measurements
$\hat{\mathbf{n}}_i$	unit vector of the measurement direction for response number i
P	number of measurement points
$p(i)$	point number i
$\mathbb{R}^3$	three-dimensional Euclidean space
s	Laplace variable
$\mathbf{t}_n(\mathbf{x}, t)$	traction vector in time domain
$\tilde{\mathbf{t}}_n(\mathbf{x}, s)$	traction vector in frequency domain
t	time
$\mathbf{u}(\mathbf{x}, t)$	three-dimensional displacement field in time domain
$\tilde{\mathbf{u}}(\mathbf{x}, s)$	three-dimensional displacement field in frequency domain
$\tilde{\mathbf{U}}^{mea}$	measured frequency domain vibration response vector
$\tilde{\mathbf{U}}^{res}$	frequency domain residual vector
$\tilde{U}_i^{mea}$	measured frequency domain vibration response number i
$\mathbf{w}^{(m)}(\mathbf{x})$	three-dimensional basis function field number m
$\mathbf{x}$	co-ordinate vector
$\boldsymbol{\varepsilon}(\mathbf{x}, t)$	Voight-matrix representation of the strain tensor in the time domain
$\tilde{\boldsymbol{\varepsilon}}(\mathbf{x}, s)$	Voight-matrix representation of the strain tensor in the frequency domain
λ	Lamés constant
v	The Poisson ratio
ρ	density

$\boldsymbol{\sigma}(\mathbf{x}, t)$	Voight-matrix representation of the Cauchy stress tensor, in the time domain
$\tilde{\boldsymbol{\sigma}}(\mathbf{x}, s)$	Voight-matrix representation of the Cauchy stress tensor, in the frequency domain
Ω	volume of the body
Ω_{fict}	volume of fictitious geometrical extension
Ω_w	volume of the body and fictitious geometrical extension
$\partial\Omega$	boundary surface of the body
ω	circular frequency
ω_m	circular eigenfrequency number m